COMPRESSION ANALYSIS TESTS FOR PROTOTYPES MADE OF DIFFERENT POLYMERS

Taher Deemyad[1], Vincent Akula[1], Anish Sebastian[1]

[1]Department of Mechanical Engineering, Idaho State University, Pocatello, ID, USA

ABSTRACT

In this paper, we tested and compared the failure loading conditions for allowed pressure over prototypes of smart toilet seats with custom shapes and materials (Polypropylene homopolymer (PPH) & Polymethyl methacrylate (PMMA)). These tests were conducted to identify the allowable maximum loading condition on these prototypes. The main challenge in designing these tests, was the application of load, specific to the custom shape of the prototype seats. A custom loading platform was designed to facilitate the application of a distributed force, to find the maximum allowable weight to identify any weak/critical sections, and failing point/s for each of the designs. However, because of the deflection of the seats, which causes a nonlinear condition for compression analysis, combined with their complex shapes, simulation of the models in SolidWorks was not very accurate. To circumvent this shortcoming an actual test bed was built and used a high accuracy electromechanical tensile & compression testing machine to subject and compare the maximum allowable loading of the seats. The results showed the seats passed the compression tests but have some differences in the locations for failures and maximum allowable pressure.

Keywords: Maximum Force, Stress Analysis, Force Analysis, Compression Analysis, Smart Toilet Seat, Nonuniform Shapes, Distributed Force, CAD Stress Analysis, PMMA, PPH, Failure Loading for Polymers

1. INTRODUCTION

Anyone who has ever used a public restroom has either an interesting or horror story to share. The cleanliness of restrooms is usually a concern for public restroom users; the issue becomes even more paramount considering the global COVID-19 pandemic. Some locations experience a higher frequency of use of their restrooms; examples include sports arenas, movie theaters, airports, etc., where regular cleaning is required to curb the spread of contagious diseases. One of the points of interest for curbing the spread diseases amongst restroom users is the toilet seats; these require regular cleaning because they are a point of contact for hundreds of users within in short period.

Given the level of technology used in day-to-day activities, manufacturers and designers are making products smarter and more autonomous [25, 26] and this affects product features like self-diagnostics for maintenance and cleaning. As a result of this, consumer goods are becoming smarter and easier to use. One of the areas which has received more attention and seen advancements recently, partly due to the COVID-19 pandemic, is cleaning/sanitizing. We are seeing smart toilet seats with the ability to self-clean or at least be cleaned in real-time by a user [1, 2]. These smart toilet seats are like the traditional ones however, there are some significant changes and new functionalities embedded in the seats. Sensors, automatic cleaning systems, and the controls are all designed to be out of sight and isolated from liquid spills or moisture. So, compared to a regular toilet seat, smart toilet seats require some kind of a cavity to house electronics and other functional systems and keep them free from moisture. This new design requirement also necessitates additional attention to materials and design of these smart toilet seats, which will insure strength and durability during normal use, especially due to varying loading conditions over the lifetime of the seat.

Recent advancements in the science of polymers have led to significant strides in strength of materials. Decreasing the weight of a material while maintaining its strength is one of the major outcomes of these improvements. Improved material properties are important to many high-tech industries such as aerospace, electronics, smart systems, and robotics. For instance, this principle is applied in designing robot manipulators with minimum actuation, where there is need to decrease the weight of the entire mechanism as much as possible and at the same time, we need a high strength structure [8, 9].

Significant research and testing contribute to determining new materials for different applications. One of the new methods for measuring the mechanical properties of materials is the micro-pillar compression test [4]. This type of test is also used to explore the deformation of plastics [5]. In the case of traditional toilet seats and the force they are subjected to when a human user

sits on them, weight is generally assumed to be applied in a normal direction to the seats' surface. So, when choosing seat materials to withstand loading, attention is paid to the maximum allowable compression [7].

Polymethyl methacrylate (PMMA) is a synthetic resin which is made from the polymerization of methyl methacrylate [10, 11]. PMMA, because of its exclusive mechanical specifications, low-cost, versatility, and reliability, is used in many different industrial applications such as being a substitute for glass in products like illuminated signs or aircraft canopies [12]. Also, it has various uses in the field of medical and orthopedics like dentures, bone implants and contact and intraocular lens [13].

In [14, 15], the uniaxial compressive stress–strain tests for PMMA for a range of loads was explained and from the experimental results, loading rate was detected as one of the main reasons for failure. In tests carried out at a higher loading rate, the material showed post-failure softening and ductile deformation. Temperature changes also had significant effect on the stress-strain response and produced thermal softening [16].

Propylene Homopolymer (PPH) is the most common grade of propylene which only contains propylene monomer. It is used mainly for packaging, textiles, healthcare, pipes, automotive, and electrical components [17]. PPH was tested in uniaxial compression at room temperature across a wide range of strain rates and results showed there is a relation between strain-rate and compressive yield stress. In addition, the medium and high-rate post-yield strain softening is maximum at the highest strain-rates [18].

Material properties play an important role in the final strength of a product, but the shape and design of a product will also have a very significant effect on improving the mechanical properties of the final design. Using curves rather than sharp edges, adding grids inside of hollow components, and using cross beams are some common methods to increase the strength of parts in a design. On the other hand, some other changes in shape and design may have significant effect in decreasing the strength of the final product. For example, dramatic change in thickness of material from one section to another or having a big difference between the size of the parts which leads to the use of sharp curves to connect them to each other.

CAD software has had improvements in recent years. Design engineers in various fields [24] employ new powerful tools to apply, simulate, and analyze the mechanical behavior under normal operating conditions of their design before making the final product. This saves money for companies because redesign and prototype manufacturing are always expensive. They use these software tools to animate dynamic models to better understand their stress-strain behavior [3]. However, it is difficult to have an accurate representation of a prototype's behavior under certain conditions.

Some complex designs are hard to simulate because of computational and software limitations. If several different materials have been used in a design and the design includes significant changes in curvature and thicknesses, then finding appropriate mesh size and proper stress-strain analysis becomes hard to accurately model/simulate.

Therefore, in cases of complicated designs with complex finite element challenges, real compression or stress tests provide a more realistic behavior-response observation and thus, more accurate results.

2. DESCRIPTION OF THE TOILET SEATS

In this project, we are comparing the maximum allowable force for two different toilet seats. Each of these seats has a different shape, size, and is made of different material. Fig. 1 shows the different views of the two seats. As it can be seen from the side view of these seats, the depth of seat #2 is less than the depth of seat #1.

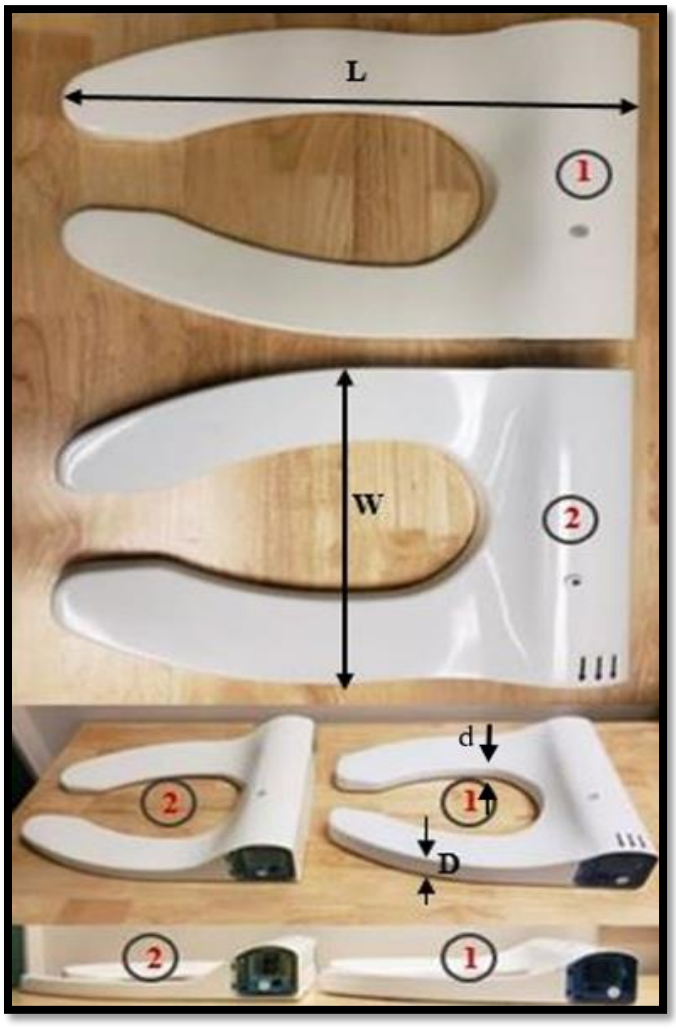

FIGURE 1: COMPARISON BETWEEN SHAPE AND SIZE OF THE SEATS #1 AND #2

Some specifications for the seats are mentioned in Table 1. From the data in the table, the maximum length (L) and width (W) for both seats are equal because the manufacturer wants this product to be used for the toilets as substitutes for standard toilet

seats. The wall thickness of Seat #1 is almost double that of seat #2.

TABLE 1: SPECIFICATIONS FOR SEATS #1 AND #2

Seats	# 1	# 2
Weight	3.064 kg	2.924 kg
Max Length (L)	0.495 m	0.495 m
Max Width (W)	0.384 m	0.384 m
Max depth (D)	0.044 m	0.0254 m
Min depth (d)	0.022 m	0.0127 m
Thickness	0.005m	0.003m
Material	Polypropylene homopolymer (PPH)	Polymethyl methacrylate (PMMA)

Seat #1 is made of Polypropylene Homopolymer (PPH) and seat #2 is made of Polymethyl methacrylate (PMMA) which are different types of plastic. Also, as it was mentioned, the depths of the seats differ. Because of the specific shape of these seats (lots of curves), this table shows just maximum depth (D) (outside) and minimum depth (d) (inside) for each of them. Although there is a significant difference in depths and thickness in these two seats, which may contribute to a difference in the volume of the material used, the weight difference is only about 100 grams. This may be because of difference in the type of materials used. The densities of the two materials are presented in the property table (Table 3). The density of material for the first seat is between 30-35% less than the density of material for the second seat. Additionally, there are some other major differences in the appearance of these two seats which may affect their strength. For instance, in the first seat, the bottom and top parts are attached to each other by screws and inside of the top part grids are used to increase the strength of the seat whereas in the second seat, the bottom and top parts are attached to each other with glue and there are no grids inside of the seat.

3. CAD MODEL FORCE AND STRESS ANALYSIS

3.1 CAD model and material selection for testing platform

Accurate stress analysis for both seats requires distributed force over the entire surface of the seats. However, because of the specific shape of the toilet seats which include many curves, it was hard to apply a distributed force. Therefore, we decided to fill out the curves with a filler material and make the entire surface flat and then put a flat steel plate on top to make sure the applied loading was uniformly distributed over the seat surface. For the filling material, the desired condition was that it should be a liquid or paste capable of filling the curved surface and forming into the desired shape. It also needed to be stronger than the seat material so that the platform does not fail prior to the seat failure. From a list of possible options, concrete was chosen as the filling material because of its high compressive strength.

All components which were included in the stress tests are shown in Fig. 2 for both seats. In the first seat, the bottom and top parts are attached to each other by screws, when in the second one they are glued to each other. Also, the counts and material for each of the components are provided in Table 1.

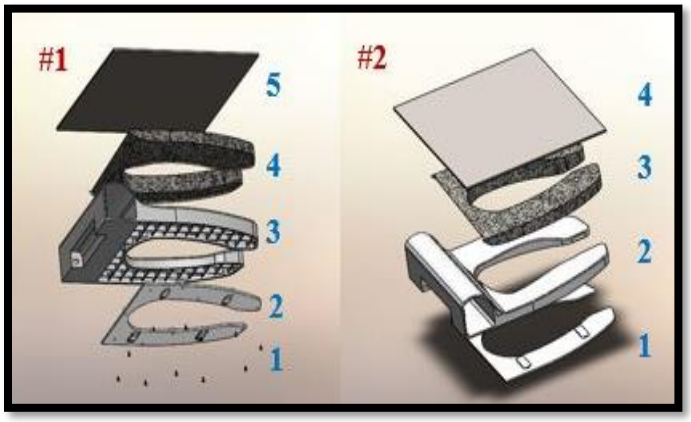

FIGURE 2: COMPONENTS FOR THE MAXIMUM FORCE TESTS

TABLE 2: NAME, QUANTITY, AND MATERIAL OF EACH PART (SEAT #1)

#	Part	QTY	Material
1	Screws	11	Steel
2	Bottom part of the seat	1	Plastic
3	Top part of the seat	1	Plastic
4	Filling material	1	Concrete
5	Top plate	1	Steel

3.2 STRESS AND FORCE ANALYSIS

In this project, we are comparing the differences in the two prototype toilet seats in size, shape, amount of material, and maximum allowable force for each of them. According to the list of heaviest people in the world [6], the maximum weight set at 1400 lbs. (635 kg). An average of between 60 to 65% of the weight of a human body is connected to the top half of the body [22]. This weight expressed as a distributed force would mostly be applied to the back section of the seat (Section A in Fig. 3). This may be true for the seating posture as shown in Fig. 3. This may not be necessarily the case for all individuals. However, if we use a high factor of safety (F.S.), in these experiments, we can assume the whole weight of body is well distributed over the seat. Therefore, to overcome this problem, we used a factor of safety of 4 in our calculations and arrived at a required tolerance of 5,600 lbs. (~25,000N). Any of these seats that can endure this amount of force will pass the stress test. Fig. 4 shows how the distributed force will be applied over the seats.

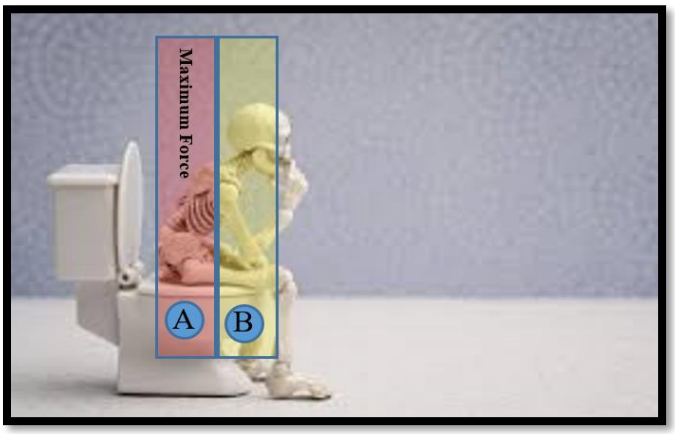

FIGURE 3: THE HUMAN ANATOMY AND THE AREA OF MAXIMUM LOAD ON A TOILET SEAT [23]

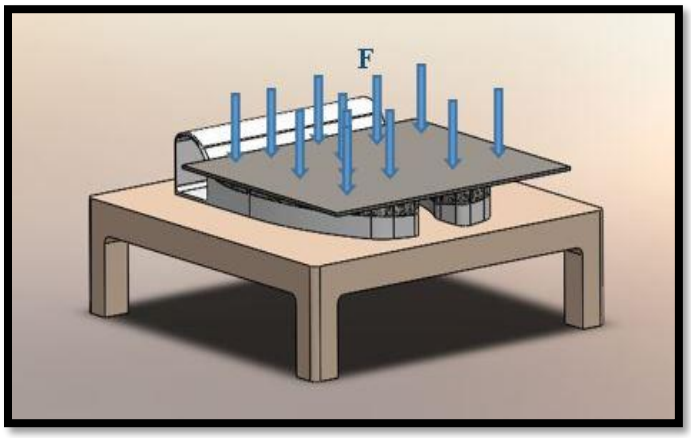

FIGURE 4: APPLYING DISTRIBUTED FORCE OVER THE SEAT

4. MODE OF FAILURE

Failure of polymers and composite materials under compressive forces can be interpreted in 2 ways: deformation and fracture. Physical deformation refers to the change in physical dimensions and shapes while fracture applies to the cracking of the piece to the point where a separation into 2 or more partially jointed or disjoint parts are noticeable [18].

Deformation includes elastic and plastic deformations and both forms can be quantified by the level of strain in the material. Fracture on the other hand is caused by static and/or impact loading. A special form of fracture which results from cyclic loading is fatigue.

Composite materials show different characteristics when under compression forces like loading. [19] describes 5 failure modes for epoxy composite under compression. Three of these modes were similar in nature, they were typified by a fracture surface parallel to the thickness and the axis of compression and perpendicular to the failure plane. This mode of failure is like the fracture failure mode described in [18]. A shear failure mode was also observed for the specimen. This involved deformation of the specimen at an angle to its thickness which is parallel to the width. Investigation of the yield behavior of PMMA under combined compression loading were recorded for normal compression [20]. In the stress-strain plot, Fig. 5 (top), similar responses are observed at different load conditions. However, when the angle of loading is altered, increase in applied force varies proportionately to displacement to a point where shearing starts to contribute to the compressive resistance of the material as shown in the load-displacement plot (bottom). The load-displacement graph provides further justification for normal loading (90°) being the ideal form to accurately estimate response for this study.

Stress-strain can be derived from (1) & (2):

$$\sigma_n = \frac{F}{A} \qquad (1)$$

$$\varepsilon_n = \frac{S}{l} \qquad (2)$$

σ_n is the normal stress and ε_n the normal strain; F, S, A and l are the load applied, displacement due to loading, initial area and length respectively.

From the experiments observed in [20], the Fig.5 shows the stress-strain response for PMMA with normal compression. The response of the material remains consistent with change in amount of load but differs with the angle of loading.

In the review of the response of PMMA to loading, it is important to highlight the effect of strain rate. Using quasi-static and dynamic experimental data, it has been observed [21] that the compressive behavior of PMMA is greatly affected by the applied strain rate and initial temperature. The study carried out by [20] shows the results at room temperature. From the study [21], Fig. 6 shows load-displacements curves of PMMA at

different strain rates. At a low strain rate, the ramp time is longer than that at a high strain rate.

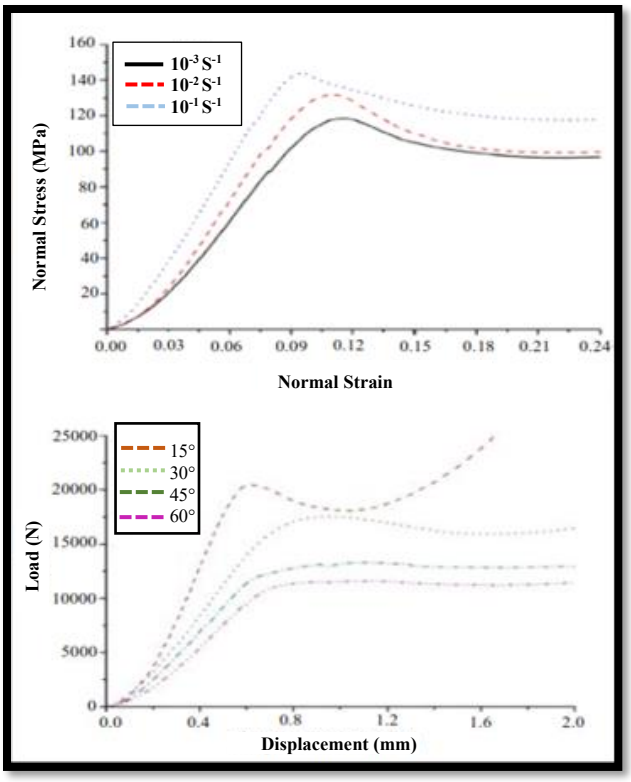

FIGURE 5: NORMAL LOADING RESPONSE GRAPH FOR PMMA [20]

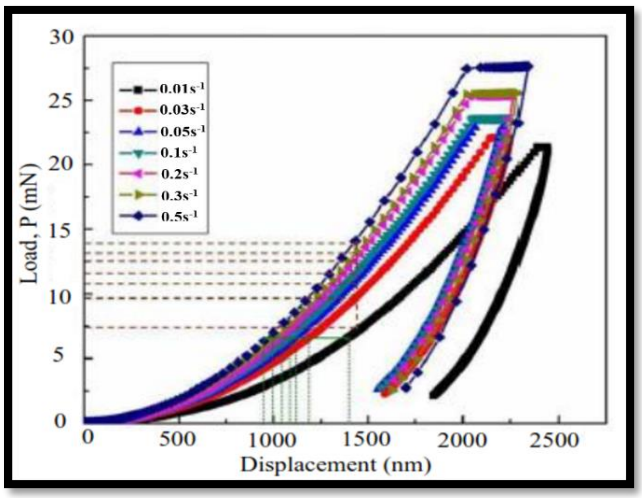

FIGURE 6: STRAIN RATE EFFECT ON COMPRESSION OF PMMA [21]

Therefore, loading intervals affect the nature of failure in PMMA and so, for our experiment, due consideration was paid to the nature of the use of the product and if rapid loading would be an issue. The tests for the study were therefore performed at room temperature with a strain rate of > $10^{-3}s^{-1}$.

5. ACTUAL TESTS

As mentioned in section II, concrete was selected for filling the curves. Some of the properties for concrete, steel, and the seat material are presented in Table 3. Observe that Seat #2 has a higher density that Seat #1. Also, we looked at the difference between Poisson's Ratios for these two materials. This suggests that material used in the second seat might more brittle. Also, both seats have a high compressive strength which is very close to the compressive strength value for concrete.

TABLE 3: SPECIFICATION OF VARIOUS MATERIALS USING IN THE TESTS

Properties	**Steel (ASTM A36)**	**Concrete**	**PPH Seat #1**	**PMMA Seat #2**
Tensile Strength (N/m^2)	4e+8	5 e+6	3.3e+7	6.1 e+7
Elastic Modulus (N/m^2)	2e+11	4.1e+10	1.79 e+9	2.77 e+9
Poisson's Ratio	0.26	0.20	0.42	0.34
Mass Density (kg/m^3)	7850	2400	933	1190
Shear Modulus (N/m^2)	7.93e+10	1.7 e+7	3.16 e+8	1.7 e+9
Compressive Strength (N/m^2)	1.52e+8	5e+7	3.93 e+7	8.3 e+7

One problem with using concrete as the inset was trying to mold it around the opening in the middle of the toilet seat. To solve this problem, we designed a mold with Styrofoam sheets and placed the Styrofoam to cover the hole and contain the movement of the concrete mix (Fig. 7).

FIGURE 7: MOLD FOR CONCRETE

As shown in Fig. 8, a thin layer would suffice for making the appropriate concrete for these tests. The concrete mixture used included half portion of gravel and half portion cement (no sand). Fig. 9 shows the toilet seat after the concrete mixture was poured in and allowed to set. This resulted in a flat surface which could now be used for the loading test.

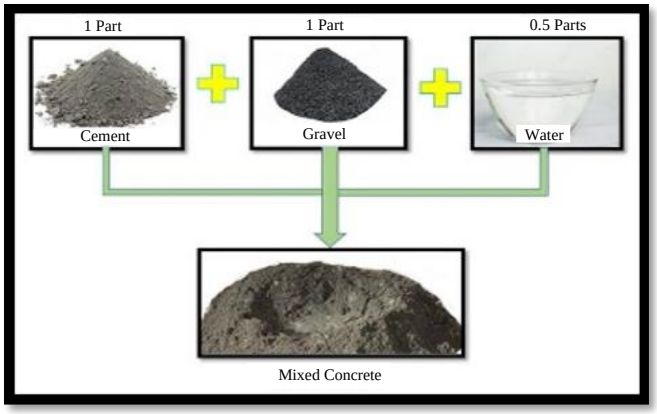

FIGURE 8: INGREDIENTS AND PROCESS OF MAKING CONCRETE

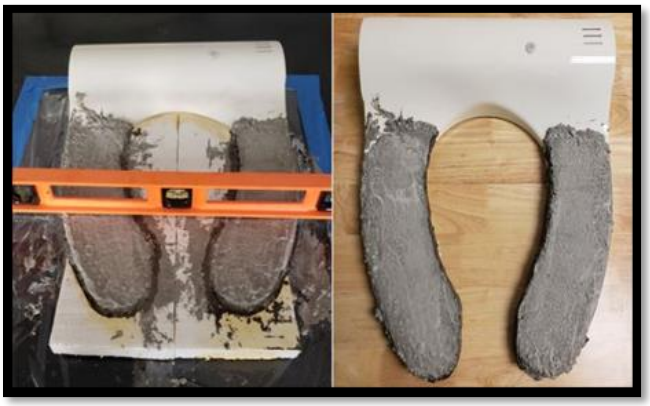

FIGURE 9: SEAT AFTER ADDING CONCRETE WITH FLAT SURFACE, READY FOR THE TEST

For the load testing we used a high accuracy electromechanical tensile & compression testing machine (Tinius Olsen) plus a compression load sensor with capacity of 225 klbf. (Interface). Fig. 10 shows the machine, sensor, and how load was applied for the seats.

6. RESULTS AND DISCUSSION

We did the compression test for both seats and analyzed the results to find the deformation, cracks, and breaking points. For seat #1 with the higher depth, the results are shown in Fig. 11. In this graph, the vertical axis is the applied force and horizontal axis is the number of steps (progress of the test based on time). From Fig. 11, first, the bumps on the bottom of the seat bend inside at applied force of around 1,200 lbs. without any crack in the seat. The seat loading was continued, the first crack appeared around 30,000 lbs. We stopped the test to check the crack and repeated the test, the next crack appeared around 40,000 lbs. Finally, the seat failed completely around 89,000 lbs.!

FIGURE 10: EECTROMECHANICAL TENSILE & COMPRESSION TESTING MACHINE (TINIUS OLSEN) AND COMPRESSION LOAD SENSOR

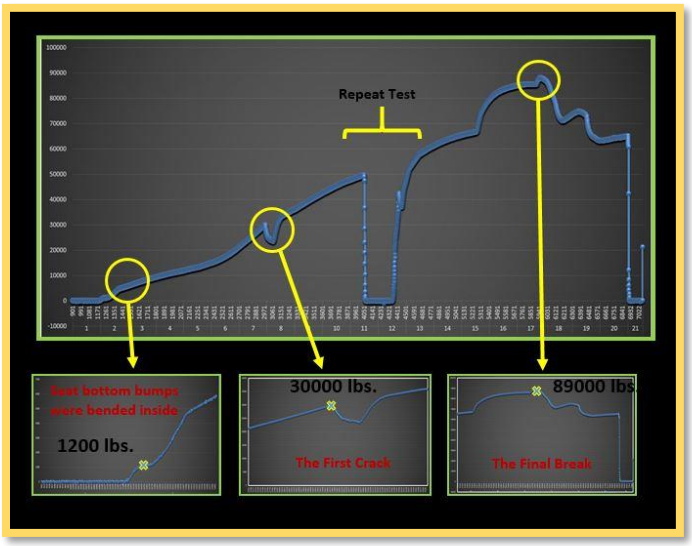

FIGURE 11: COMPRESSION TEST RESULTS FOR THE SEAT #1

Slide #1 in Fig. 12 shows the bumps on bottom of the seat which bent inwards first, and eventually failed completely. The other five slides show the major breaking points on the seat. As it can be seen the major cracks happened on inside and outside of the arms and back part of the seat, bottom edges, and bumps on the bottom of the seat.

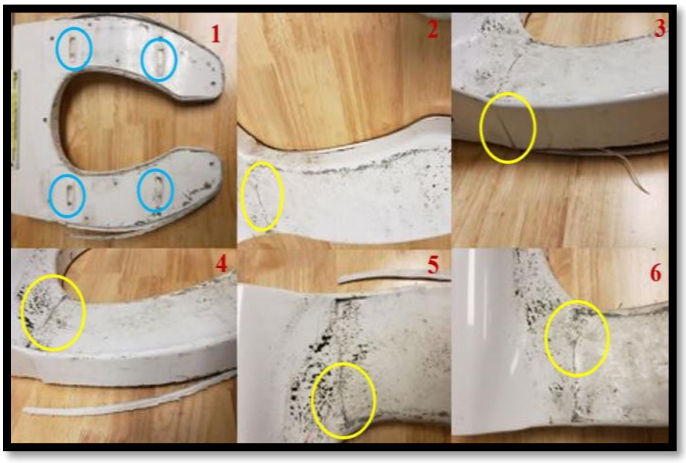

FIGURE 12: CRACK AND BREAKING POINTS IN THE SEAT #1

The results for the second seat were completely different. Fig. 13 shows the results for seat #2. As can be seen, the failure behavior is similar as the previous test, first the bumps on the bottom of the seat bend inwards but this time at 800 lbs. There were no visible cracks on the surface at this point. After checking the seat for any possible cracks, we repeated the test but this seat without any small crack like the first test, suddenly failed completely at around 6,800 lbs.

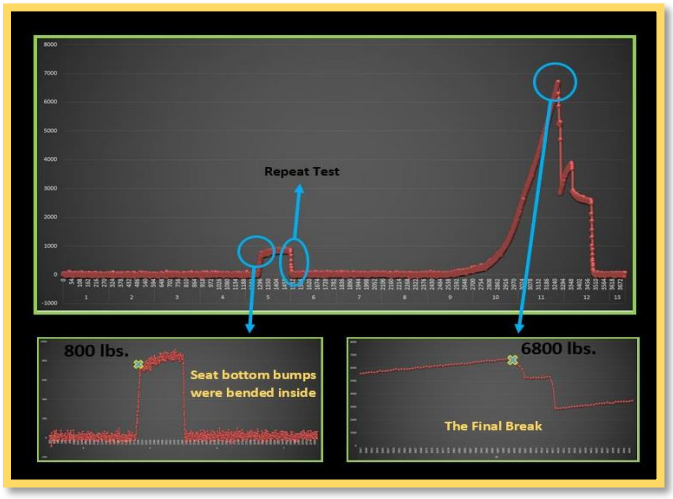

FIGURE 13: COMPRESSION TEST RESULTS FOR THE SEAT #2

This time all the major breaking points occurred at the connection between the arms and back of the seat (main body). We did not notice any breaks or cracks on the bumps and bottom part of the seat, as in the first case Fig. 14 shows the breaking points of seat #2.

FIGURE 14: CRACK AND BREAKING POINTS IN THE SEAT #2

According to the tests results, there are some important outcomes. First of all, both seats are able to pass the compression test because the first crack or break in them happened over 5,600 lbs. which is the maximum force that can be applied by a human which has been calculated based on a F.S. of 4! Secondly, seat #1 failed at a much higher load as compared to seat #2. There are several different reasons which might have affected this outcome. It could be a result of the material used to make the seats (seat #2 is made of a more fragile material), there are sharp changes in depth of the arms and main body in the second seat which creates stresses at those points (seat #2 exactly broke at that point), there are no grids in between the bottom and top part of the seat, for the second seat. Other design difference which may have contributed to the different failure locations could be the use of plates with less thickness for the second seat, less depth of the arms, and the use of glue rather than screws to connect the top and the bottom part of the seat.

However, there are some advantages for seat #2. Seat #2 has an aesthetically more pleasing appearance as compared to seat #1, the weight of seat #2 is less than seat #1 which makes it easier for users to lift it up. Also, the lower weight will help in the longevity of the soft hinges used for the prototypes. Manufacturing seat#2 requires less materials which will help bring down the overall process of the smart seat benefitting both, the business and the costumers. Also, if we look at it from an environmental perspective lesser material means lesser material going to the landfills.

7. CONCLUSION

In this paper, compression analysis for two different toilet seat prototypes were studied. Each of these seats had different shape, weight, and were made of different materials. Because of unique shape of the smart toilet seats which house the cleaning solution and the electronics, the seat design included lots of curved surfaces. To test the failure loading conditions of the seats, we filled the curves with concrete to apply loads vertically. Final results showed both seats are able to endure the maximum weight of a human with a factor of safety of 4 about 5,600 lbs. Seat prototype 1 was capable of carrying much more weight compared to seat prototype 2. However, the design of the seat with less weight tolerance has advantages over seat prototype 1.

REFERENCES

[1] F. Shaikh, F. Shaikh, K. Sayed, N. Mittha, and N. Khan, 2019, March. Smart Toilet Based On IoT. In 2019 3rd International Conference on Computing Methodologies and Communication (ICCMC) (pp. 248-250). IEEE.

[2] S. Maric, J. Phelps, Z.M. Bzymek, and V. Moreno, 2016, November. Design and Fabrication of a Self-Cleaning Toilet: Developing a Student Invention. In ASME International Mechanical Engineering Congress and Exposition (Vol. 50571, p. V005T06A014). American Society of Mechanical Engineers.

[3] T. Deemyad, R. Moeller, and A. Sebastian. "Chassis Design and Analysis of an Autonomous Ground Vehicle (AGV) using Genetic Algorithm". In Intermountain Engineering, Technology, and Computing Conference (i-ETC). IEEE, 2020.

[4] H. Fei, A. Abraham, N. Chawla, and H. Jiang (September 17, 2012). "Evaluation of Micro-Pillar Compression Tests for Accurate Determination of Elastic-Plastic Constitutive Relations." ASME. J. Appl. Mech. November 2012; 79(6): 061011

[5] X. Fang, M. Rasinski, A. Kreter, C. Kirchlechner, C. Linsmeier, G. Dehm, and S. Brinckmann, 2019. Plastic deformation of tungsten due to deuterium plasma exposure: Insights from micro-compression tests. Scripta Materialia, 162, pp.132-135.

[6] T.J. Sanders, and M.A. Gernsbacher, 2004. Accessibility in text and discourse processing. Discourse Processes, 37(2), pp.79-89.

[7] W. Chen, F. Lu, and M. Cheng, 2002. Tension and compression tests of two polymers under quasi-static and dynamic loading. Polymer testing, 21(2), pp.113-121.

[8] T. Deemyad, N. Hassanzadeh, and A. Perez-Gracia. Coupling mechanisms for multi-fingered robotic hands with skew axes. In Mechanism Design for Robotics (MEDER). Springer, 2018.

[9] T. Deemyad, O. Heidari, and A. Perez-Gracia. Singularity Design for RRSS Mechanisms. In USCToMM Symposium on Mechanical Systems and Robotics (MSR) Conferences. Springer, 2020.

[10] G. Chen, W. Yuan, Y. Bai, W. Zhao, J. Zhang, Y. Wu, X. Gu, S. Chen, and H. Yu, 2018. Synthesis of pour point depressant for heavy oil from waste organic glass. Petroleum Chemistry, 58(1), pp.85-88.

[11] N.H. Manab, E. Baharudin, F.C. Seman, and A. Ismail, 2018, December. 2.45 GHz Patch Antenna Based on Thermoplastic Polymer Substrates. In 2018 IEEE International RF and Microwave Conference (RFM) (pp. 93-96). IEEE.

[12] M.F. Adnan, 2013. The Effect of Temperature on Polymethyl Methacrylate Acrylic (PMMA) (Doctoral dissertation, UMP).

[13] R.Q. Frazer, R.T. Byron, P.B. Osborne, and K.P. West, 2005. PMMA: an essential material in medicine and dentistry. Journal of long-term effects of medical implants, 15(6).

[14] Z. Zhou, B. Su, Z. Wang, Z. Li, X. Shu, and L. Zhao, 2013. Shear-compression failure behavior of PMMA at different loading rates. Materials Letters, 109, pp.151-153.

[15] A.D. Mulliken, and M.C. Boyce, 2006. Mechanics of the rate-dependent elastic–plastic deformation of glassy polymers from low to high strain rates. International journal of solids and structures, 43(5), pp.1331-1356.

[16] E.M. Arruda, M.C. Boyce, and R. Jayachandran, 1995. Effects of strain rate, temperature and thermomechanical coupling on the finite strain deformation of glassy polymers. Mechanics of Materials, 19(2-3), pp.193-212.

[17]https://www.machinedesign.com/community/article/21837192/whats-the-difference-between-polypropylene-types#:~:text=Different%20Types%20of%20Polypropylene&text=Propylene%20homopolymer%20is%20the%20most,%2C%20automotive%2C%20and%20electrical%20applications.

[18] N. E Dowling, 2013. Mechanical Behavior of Materials, Fourth Edition p 118-146

[19] E. M. Odom, and D. F. Adams, 1990. Failure Modes of Unidirectional Carbon/Epoxy Composite Compression Specimens. Composites Volume 21, No 4 July 1990. Pp 289-296.

[20] j. Zhang, T. Jin, Z. Wang, and L. Zhao, 2016. Experimental investigation on yield behavior of PMMA under combined shear–compression loading. 2016 Published by Elsevier B.V. This is an open access article under the CC BY-NC-ND license (http://creativecommons.org/licenses/by-nc-nd/4.0/)

[21] M. Nasraoui, P. Forquin, L. Siad, and A. Rusinek, 2011. Influence of strain rate, temperature and adiabatic heating on the mechanical behaviour of poly-methyl-methacrylate: Experimental and modelling analyses. 2011 Elsevier Ltd. All rights reserved. doi:10.1016/j.matdes.2011.11.032

[22] https://exrx.net/Kinesiology/Segments

[23]https://depositphotos.com/stock-photos/skeleton-on-toilet.html

[24] S. Habibian, M. Dadvar, B. Peykari, A. Hosseini, M.H. Salehzadeh, A.H. Hosseini, and F. Najafi, 2021. Design and implementation of a maxi-sized mobile robot (Karo) for rescue missions. ROBOMECH Journal, 8(1), pp.1-33.

[25] K. Majd, M. Razeghi-Jahromi and A. Homaifar, "A stable analytical solution method for car-like robot trajectory tracking and

optimization," in *IEEE/CAA Journal of Automatica Sinica*, vol. 7, no. 1, pp. 39-47, January 2020, doi: 10.1109/JAS.2019.1911816.

[26] K. Majd, S. Yaghoubi, T. Yamaguchi, B. Hoxha, D. Prokhorov, and G. Fainekos, 2021. Safe Navigation in Human Occupied Environments Using Sampling and Control Barrier Functions. arXiv preprint arXiv:2105.01204.